

## Parallel Framework for Complex Reservoir Simulation with Advanced Discretization and Linearization Schemes

Li, Longlong; Khait, Mark; Voskov, Denis; Abushaikha, Ahmad

**DOI**

[10.2118/200615-MS](https://doi.org/10.2118/200615-MS)

**Publication date**

2020

**Document Version**

Final published version

**Published in**

SPE Europec Featured at 82nd EAGE Conference and Exhibition

**Citation (APA)**

Li, L., Khait, M., Voskov, D., & Abushaikha, A. (2020). Parallel Framework for Complex Reservoir Simulation with Advanced Discretization and Linearization Schemes. In *SPE Europec Featured at 82nd EAGE Conference and Exhibition: 8-11 December, Amsterdam, The Netherlands* (pp. 1-14). Article SPE-200615-MS (Society of Petroleum Engineers - SPE Europec Featured at 82nd EAGE Conference and Exhibition). Society of Petroleum Engineers. <https://doi.org/10.2118/200615-MS>

**Important note**

To cite this publication, please use the final published version (if applicable). Please check the document version above.

**Copyright**

Other than for strictly personal use, it is not permitted to download, forward or distribute the text or part of it, without the consent of the author(s) and/or copyright holder(s), unless the work is under an open content license such as Creative Commons.

**Takedown policy**

Please contact us and provide details if you believe this document breaches copyrights. We will remove access to the work immediately and investigate your claim.

***Green Open Access added to TU Delft Institutional Repository***

***'You share, we take care!' - Taverne project***

**<https://www.openaccess.nl/en/you-share-we-take-care>**

Otherwise as indicated in the copyright section: the publisher is the copyright holder of this work and the author uses the Dutch legislation to make this work public.

**SPE-200615-MS**

## **Parallel Framework for Complex Reservoir Simulation with Advanced Discretization and Linearization Schemes**

Longlong Li, Division of Sustainable Development, College of Science and Engineering, Hamad Bin Khalifa University; Mark Khait and Denis Voskov, TU Delft; Ahmad Abushaikha, Division of Sustainable Development, College of Science and Engineering, Hamad Bin Khalifa University

Copyright 2020, Society of Petroleum Engineers

This paper was prepared for presentation at the SPE Europec featured at 82nd EAGE Conference and Exhibition originally scheduled to be held in Amsterdam, The Netherlands, 8-11 June 2020. The physical event was postponed until 14-17 June 2021. A virtual SPE Europec was held 1-3 December 2020 for SPE authors to present their papers. The official proceedings were published online on 8 June 2020.

This paper was selected for presentation by an SPE program committee following review of information contained in an abstract submitted by the author(s). Contents of the paper have not been reviewed by the Society of Petroleum Engineers and are subject to correction by the author(s). The material does not necessarily reflect any position of the Society of Petroleum Engineers, its officers, or members. Electronic reproduction, distribution, or storage of any part of this paper without the written consent of the Society of Petroleum Engineers is prohibited. Permission to reproduce in print is restricted to an abstract of not more than 300 words; illustrations may not be copied. The abstract must contain conspicuous acknowledgment of SPE copyright.

---

### **Abstract**

The continuous progress of reservoir monitoring technology provides encouraging capacities to reduce uncertainties in the subsurface characterization and to mitigate risks in field development applying the reservoir simulation approach. However, it is always challenging to take full advantage of the observation data, since an accurate representation of strong heterogeneities requires a high-resolution grid. Most of the discretization methods cannot handle full tensor permeability, and high nonlinearity introduced by complex physical process drastically reduces simulation efficiency. In this work, we develop an advanced parallel framework for reservoir simulation with the implementation of state of the art discretization and linearization methods. We apply the multipoint flux approximation (MPFA) method to handle the full tensor permeability in unstructured grids. To keep the fidelity of the geological model and improve computational efficiency, we use massively parallel computations via Message Passing Interface (MPI). Complex subsurface physics is described by mass-based formulations making the framework flexible for general-purpose reservoir simulation. However, the representation of phase behavior introduces additional workload when compared with the phase-based formulations in the traditional approach. Here, we apply the Operator-Based Linearization (OBL) approach which not only overcomes this drawback but also turns it to an advantage. In this method, the conservation equations are described in an operator form. By constructing a library of tabulated operators, the repeated work spent on complex phase behavior and property evaluation can be significantly reduced. We benchmark the parallel framework with analytical solutions under single-phase flow and multiphase flow. The results demonstrate that the parallel framework provides accurate simulation results for structured and unstructured grids. We validate that MPFA implemented in our parallel framework converges to real solutions when the permeability is a full tensor. Besides, several realistic cases have been rigorously tested confirming high computational capacity, efficiency, and accuracy of the advanced massively parallel framework for general-purpose reservoir simulation. With the implementation of MPFA and OBL approaches, the parallel framework is fully equipped for the simulation of problems with full tensor permeability, high-heterogeneities, and complex physical processes.

## Introduction

With the development of reservoir monitoring technology, more valuable data has been observed during the exploration and development stages. Assisted with reservoir simulation, this data can help to reduce uncertainties in the subsurface characterization and mitigate risks in field development. However, it is always challenging to integrate detailed information into reservoir simulation. For example, limited by the computational efficiency, a highly heterogeneous geological model can not be applied for reservoir simulation of complex physical processes (e.g. compositional simulation) directly.

The most popular approach to reducing the number of degrees of freedom is a coarsening of geological models which increases numerical errors inevitably. However, another challenge may be introduced after the upscaling procedure due to the appearance of full tensor permeability. The most commonly used two-point flux approximation (TPFA) method can not provide convergent solutions for reservoirs with full permeability tensor [Abushaikh et al., 2017; Hjeij and Abushaikh 2019a and b]. Also, the solutions using the TPFA method are not always numerically convergent for general unstructured grid cases [Abushaikh et al., 2020]. Besides, the complex physics of multiphase flow makes it hard for the development of a reservoir simulator and enhances the nonlinearity of the system which can drastically reduce simulation efficiency. Thus, an accurate and computationally efficient reservoir simulator is still strongly required.

To overcome the limitations introduced by TPFA and to have a better understanding of the flow behavior in the subsurface domain, several advanced numerical methods have been developed in reservoir simulation [Aavatsmark et al., 1998; Aavatsmark, 2002; Abushaikh et al., 2015; Abushaikh et al., 2018; Hjeij et al. 2019a; Hjeij et al. 2019b; Zhang et al., 2019a; Zhang et al., 2019b]. Among them, the O-method of multipoint flux approximation (MPFA-O) has been proved to be an efficient and convergent method. The flow behavior in strong heterogeneities [Abushaikh et al., 2008; Li et al., 2014; Wang et al., 2019; Li et al., 2018a; Wu et al., 2018] and the effect of phase behavior on flow response [Voskov et al. 2008; Voskov et al. 2009; Li et al., 2016; Liu et al., 2018; Li et al., 2018b] have also been widely discussed.

In this work, we introduce an advanced parallel framework for reservoir simulation. We apply the MPFA-O method on a general unstructured grid and compare results with the TPFA approach. We demonstrate that our framework can provide convergent solutions for the cases with full tensor permeability and unstructured grid. For high-fidelity geological models, we use massively parallel computations via Message Passing Interface (MPI) which can improve the simulation efficiency significantly. To make the framework more general, we apply the mass-based formulations which unify the single-phase, dead oil, black oil, and the compositional models.

For the solution of the nonlinear governing equations, we apply the state of art linearization method named as operator-based linearization (OBL) [Voskov, 2017; Khait et al., 2017; Khait et al., 2018a; Khait et al., 2018b]. With the application of OBL, the phase behavior computation workload can be drastically reduced. Also, it simplifies the programming of Jacobian assembly which in turn improves the flexibility of the simulation framework. We benchmark the numerical solutions with analytical solutions under single-phase flow and multiphase flow conditions. The results demonstrate that the parallel framework developed in this work is capable to provide accurate and efficient solutions for reservoir simulation. The simulations of a highly heterogeneous geo-model on different numbers of processors demonstrate the strong scalability of the parallel framework.

## Parallel Framework for Reservoir Simulation

In this section, we describe the governing equations, discretization method, linearization method, and the implementation of massively parallel computation.

## Modelling approach

Assuming that there are  $n_c$  components and  $n_p$  phases in an isothermal system, the transport equations can be written as below.

$$\frac{\partial}{\partial t} \left( \phi \sum_{j=1}^{n_p} x_{cj} \rho_j s_j \right) + \operatorname{div} \sum_{j=1}^{n_p} x_{cj} \rho_j \mathbf{u}_j + \sum_{j=1}^{n_p} x_{cj} \rho_j \tilde{q}_j = 0, \quad c = 1, \dots, n_c. \quad (1)$$

Here,  $\phi$  is the reservoir porosity;  $t$  is the time; subscript  $c$  is the index for mass components; subscript  $j$  is the index for phases;  $x_{cj}$  is the mole fraction of component  $c$  in phase  $j$ ;  $\rho$  is the phase molar density;  $s$  is the saturation;  $\tilde{q}$  is the phase rate per unit volume.  $\mathbf{u}_j$  is the Darcy velocity of phase  $j$ :

$$\mathbf{u}_j = - \left( \mathbf{K} \frac{k_{rj}}{\mu_j} \nabla P \right), \quad j = 1, \dots, n_p \quad (2)$$

where  $\mathbf{K}$  is the permeability tensor;  $k_{rj}$  is the relative permeability of phase  $j$ ;  $\mu$  is the viscosity;  $P$  is the pressure.

There are two kinds of formulations, including mass-based and phase-based formulations, used for solving the system of governing equations. In this study, to unify the formulations of the single-phase, dead oil, black oil, and the compositional models, we apply the mass-based formulations of which the unknowns are pressure and overall compositions  $z_c = \sum_j x_{cj} \rho_j s_j / \sum_j \rho_j s_j$ .

## Multipoint flux approximation method

As a common discretization method, the TPFA method is widely used in many reservoir simulators. However, it is limited to provide an accurate solution for the simulations which apply unstructured grid or full tensor permeability. To handle these two situations, by using functions related to geometry calculation in INMOST (Terekhov et al., 2019), we apply the MPFA-O method for discretization. As shown in Figure 1, there are six control volumes in black bold lines and two intersection volumes in red lines.  $x_1, x_2, x_3, x_4, x_5,$  and  $x_6$  are the centers of cell 1, cell 2, cell 3, cell 4, cell 5, and cell 6;  $x_1^-, x_2^-, x_3^-, x_4^-, x_5^-, x_6^-$  and  $x_7^-$  are the midpoints of edges. The fluxes through half-edges including  $x_1^-x_7^-, x_3^-x_7^-, x_7^-x_2^-$  and  $x_7^-x_4^-$  are computed through intersection volume  $x_1x_2x_4x_3$ , and the fluxes through half-edges including  $x_2^-x_8^-, x_6^-x_8^-, x_8^-x_5^-$  and  $x_8^-x_7^-$  are computed through intersection volume  $x_3x_4x_6x_5$ .

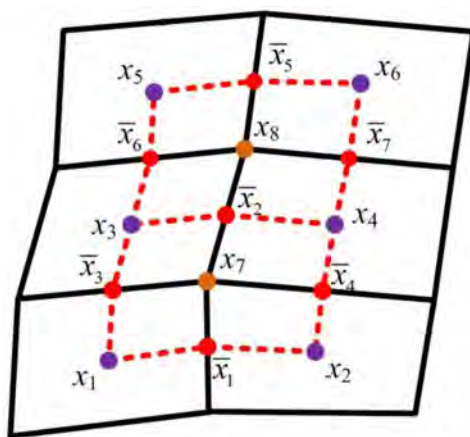


Figure 1—The schematic of control volumes and intersection volumes

As shown in Figure 2,  $\mathbf{v}_1^{(1)}$  is the normal on the connection line between  $x_1$  and  $x_3$ , the superscript denotes the index of cell 1;  $\mathbf{n}_1$ ,  $\mathbf{n}_2$ ,  $\mathbf{n}_3$ , and  $\mathbf{n}_4$  are the normal vectors on the half-edges. In the sub-region of the intersection volume, the gradient of potential can be written as:

$$\text{grad } P = \frac{1}{2F_1} \left[ \mathbf{v}_1^{(1)} (P_1 - P_1) + \mathbf{v}_2^{(1)} (P_3 - P_1) \right] \quad (3)$$

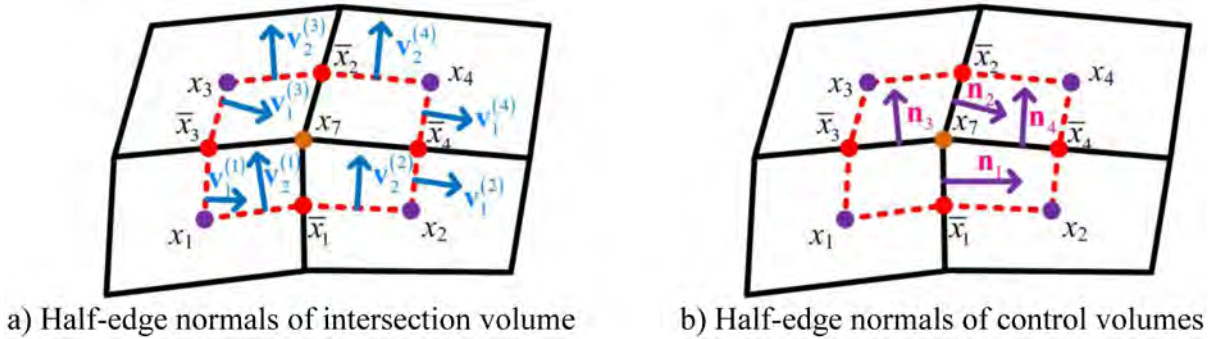


Figure 2—Normal vectors in an interaction volume

where  $F_1$  is the area of the triangle  $x_1 x_2 x_3$ .

The flux through half-edge is represented by  $f_i^{(k)}$  where  $i$  is the index of the edge and  $k$  is the index of the cell. Take the cell 1 for example, the fluxes through half-edges can be written as:

$$\begin{bmatrix} f_1^{(1)} \\ f_3^{(1)} \end{bmatrix} = - \begin{bmatrix} \Gamma_1 \mathbf{n}_1^T \\ \Gamma_3 \mathbf{n}_3^T \end{bmatrix} \mathbf{K}_1 \text{grad } P = - \frac{1}{2F_1} \begin{bmatrix} \Gamma_1 \mathbf{n}_1^T \\ \Gamma_3 \mathbf{n}_3^T \end{bmatrix} \mathbf{K}_1 \begin{bmatrix} \mathbf{v}_1^{(1)} & \mathbf{v}_2^{(1)} \\ P_1 - P_1 & P_3 - P_1 \end{bmatrix} \quad (4)$$

where  $\mathbf{K}_1$  is the permeability of cell 1 in full tensor format;  $\Gamma$  is the length of half-edge.

By defining  $G_1$

$$G_1 = \frac{1}{2F_1} \begin{bmatrix} \Gamma_1 \mathbf{n}_1^T \\ \Gamma_3 \mathbf{n}_3^T \end{bmatrix} \mathbf{K}_1 \begin{bmatrix} \mathbf{v}_1^{(1)} & \mathbf{v}_2^{(1)} \end{bmatrix} = \frac{1}{2F_1} \begin{bmatrix} \Gamma_1 \mathbf{n}_1^T \mathbf{K}_1 \mathbf{v}_1^{(1)} & \Gamma_1 \mathbf{n}_1^T \mathbf{K}_1 \mathbf{v}_2^{(1)} \\ \Gamma_3 \mathbf{n}_3^T \mathbf{K}_1 \mathbf{v}_1^{(1)} & \Gamma_3 \mathbf{n}_3^T \mathbf{K}_1 \mathbf{v}_2^{(1)} \end{bmatrix} \quad (5)$$

equation (4) can be written as

$$\begin{bmatrix} f_1^{(1)} \\ f_3^{(1)} \end{bmatrix} = -G_1 \begin{bmatrix} P_1 - P_1 \\ P_3 - P_1 \end{bmatrix} \quad (6)$$

By using the same approach, we can obtain matrixes  $G_2$ ,  $G_3$ , and  $G_4$ . The fluxes through half-edges in each cell can be written as:

$$\begin{bmatrix} f_1^{(1)} \\ f_3^{(1)} \end{bmatrix} = -G_1 \begin{bmatrix} P_1 - P_1 \\ P_3 - P_1 \end{bmatrix}, \begin{bmatrix} f_1^{(2)} \\ f_4^{(2)} \end{bmatrix} = -G_2 \begin{bmatrix} P_2 - P_1 \\ P_4 - P_2 \end{bmatrix} \quad (7)$$

$$\begin{bmatrix} f_2^{(3)} \\ f_3^{(3)} \end{bmatrix} = -G_3 \begin{bmatrix} P_2 - P_3 \\ P_3 - P_3 \end{bmatrix}, \begin{bmatrix} f_2^{(4)} \\ f_4^{(4)} \end{bmatrix} = -G_4 \begin{bmatrix} P_4 - P_2 \\ P_4 - P_4 \end{bmatrix}$$

By assuming that the flux on the interface of two neighboring cells is continuous, equation (7) can be rewritten as:



$$\begin{aligned}
f_1 &= -g_{1,1}^{(1)}(\bar{P}_1 - P_1) - g_{1,2}^{(1)}(\bar{P}_3 - P_1) = g_{1,1}^{(2)}(\bar{P}_1 - P_2) - g_{1,2}^{(2)}(\bar{P}_4 - P_2) \\
f_2 &= g_{1,1}^{(4)}(\bar{P}_2 - P_4) + g_{1,2}^{(4)}(\bar{P}_4 - P_4) = -g_{1,1}^{(3)}(\bar{P}_2 - P_3) + g_{1,2}^{(3)}(\bar{P}_3 - P_3) \\
f_3 &= -g_{2,1}^{(3)}(\bar{P}_2 - P_3) + g_{2,2}^{(3)}(\bar{P}_3 - P_3) = -g_{2,1}^{(1)}(\bar{P}_1 - P_1) - g_{2,2}^{(1)}(\bar{P}_3 - P_1) \\
f_4 &= g_{2,1}^{(2)}(\bar{P}_1 - P_2) - g_{2,2}^{(2)}(\bar{P}_4 - P_2) = g_{2,1}^{(4)}(\bar{P}_2 - P_4) + g_{2,2}^{(4)}(\bar{P}_4 - P_4)
\end{aligned} \tag{8}$$

By defining  $\mathbf{f} = [f_1, f_2, f_3, f_4]^T$ ,  $\mathbf{P} = [P_1, P_2, P_3, P_4]^T$ ,  $\bar{\mathbf{P}} = [\bar{P}_1, \bar{P}_2, \bar{P}_3, \bar{P}_4]^T$ , we can obtain two equations:

$$\mathbf{f} = \mathbf{C}\bar{\mathbf{P}} + \mathbf{F}\mathbf{P}. \tag{9}$$

$$\mathbf{A}\bar{\mathbf{P}} = \mathbf{B}\mathbf{P}. \tag{10}$$

By combining equations (9) and (10), we can obtain:

$$\mathbf{f} = \mathbf{T}\mathbf{P}, \quad \mathbf{T} = \mathbf{C}\mathbf{A}^{-1}\mathbf{B} + \mathbf{F}. \tag{11}$$

As  $\mathbf{T}$  is computed based on intersection volume, it can only be used to compute the fluxes through half-edges. To simplify the Jacobian assembly, we integrate the  $\mathbf{T}$  of intersection volumes as connection-based transmissibility vector. For example, in Figure 1, we get a vector  $\mathbf{T}_{integ} = [T_1 \ T_2 \ T_3 \ T_4 \ T_5 \ T_6]$  for the connection between cell 3 and cell 4. With the vector of pressure  $\mathbf{P} = [P_1 \ P_2 \ P_3 \ P_4 \ P_5 \ P_6]^T$ , we get the flux through edge  $x_7x_8$  by  $flux_{x_7x_8} = \mathbf{T}_{integ} \cdot \mathbf{P}$ . Thus, by applying the MPFA-O method to discretize the mesh and applying backward Euler approximation to discretize in time, the governing equations can be transformed as:

$$\left( V\phi \sum_{j=1}^{n_p} x_{c,j} \rho_j s_j \right)^{n+1} - \left( V\phi \sum_{j=1}^{n_p} x_{c,j} \rho_j s_j \right)^n - \Delta t \sum_l \left( \sum_{j=1}^{n_p} x_{c,j}^l \rho_j^l \lambda_j^l \mathbf{T}_{integ}^l \mathbf{P} \right) + \Delta t \sum_{j=1}^{n_p} x_{c,j} \rho_j q_j = 0, \quad c = 1, \dots, n_c. \tag{12}$$

Here  $V$  is the volume of a control volume;  $l$  denotes the edges/faces of a control volume;  $\lambda_j^l = (k_{rj} / \mu_j)^l$  is the mobility of phase  $j$  over the interface  $l$  by upstream weighting,  $q_j = q_j V$  is the source of phase  $j$ ;  $n+1$  is the current time step;  $n$  is the previous time step.

### Operator-based linearization method

As an unconditionally stable method, the implicit method has been implemented in many reservoir simulators. However, it is always challenging to construct the Jacobian matrix, especially when the phase behavior is complex. In general, the main challenges are introduced by properties and their derivatives. During a simulation run, properties may be computed multiple times for the same state of the system (similar values of nonlinear unknowns). The repeated work reduces the simulation efficiency a lot.

There are three ways to determine the derivatives including numerical approach, straightforward hand-differentiation approach, and automatic differentiation techniques. The numerical approach is quite flexible but often fails to offer a robust solution and can be expensive for multicomponent systems [Pruess et al., 1999; Pruest, 2004]. The straightforward hand-differentiation approach is the most accurate strategy and is implemented in many commercial simulators. However, the ensemble of the Jacobian becomes quite complex which usually reduces the flexibility to add/change governing physics in the simulation framework [Cao, 2002]. The automatic differentiation techniques [Voskov 2012; Zaydullin et al. 2014; Garipov et al. 2016; Garipov et al. 2018] are proved to provide robust solutions and help to keep the flexibility of a reservoir simulator. However, the automatic differentiation usually introduces an overhead and limits the efficiency of a reservoir simulator.

In this work, we apply the state-of-the-art operator-based linearization (OBL) method proposed by Voskov (2017). By using the OBL, equations (12) are transformed in an operator format:

$$r_c(\xi, \omega, \mathbf{u}) = V(\xi) \phi_0(\xi) [\alpha_c(\omega) - \alpha_c(\omega_n)] - \sum_i \Delta t \mathbf{T}_{integ}^l \mathbf{P} \beta_c^l(\omega) + \theta_c(\xi, \omega, \mathbf{u}), \quad c = 1, \dots, n_c \quad (13)$$

where, the operators are defined as:

$$\alpha_c(\omega) = [1 + c_r(P - P_{ref})] \sum_{j=1}^{np} x_{cj} \rho_j s_j \quad (14)$$

$$\beta_c(\omega) = \sum_{j=1}^{np} x_{cj}^l \rho_j^l \lambda_j^l \quad (15)$$

$$\theta_c(\xi, \omega, \mathbf{u}) = \Delta t \sum_{j=1}^{np} x_{cj} \rho_j q_j(\xi, \omega, \mathbf{u}) \quad (16)$$

Here,  $P_{ref}$  is the reference pressure for the porosity  $\phi_0$ . From equations (14) to (16),  $\alpha_c$  and  $\beta_c$  are only dependent on the phase and rock properties and independent of spatially distributed properties. The term  $\theta_c$  can also be separated into space-dependent and state-dependent operators, but considering the complexity of the well conditions, we do not show it here. Therefore, the most severe nonlinearity and complexity related to phase behavior and property calculation are introduced by  $\alpha_c$ ,  $\beta_c$  and their derivatives.

In the OBL, the parameter space of the nonlinear unknowns of  $\alpha_c$  and  $\beta_c$  are discretized using a uniform grid. Once a status falls inside a hypercube with certain coordinates, we compute the operators on the vertices of this hypercube. Then, the operators and their derivatives inside the hypercube can be determined by interpolation. To save the workload spent on operator computation, the operators on each node are only computed single time and stored. The robustness and reliability of the OBL approach have already been proofed in multiple numerical studies (Voskov, 2017; Khait and Voskov, 2017; 2018a, b). In addition, the utilization of the OBL approach simplifies the programming of the linearization stage which makes the simulator more general and flexible.

### Implementation of massively parallel computation

As an efficient and promising approach to improve computational performance, the massively parallel computation is chosen as a base technology for our reservoir simulation framework. To utilize that, we should first assign workload to the processors on cluster nodes evenly. As schematically shown in Figure 3a, a geo-model with  $8 \times 8$  grids is divided into four sub-domains through reservoir domain decomposition. Then we determine shared cells in blue (Figure 3b) and ghost cells in red (Figure 3c) in each sub-domain. By assigning the grids in each sub-domain to a unique processor, the assignment of the workload is completed. Next, during a simulation run, to integrate the workload of each sub-domain, we apply the Message Passing Interface (MPI) to exchange the information among different processors by sharing the variables of shared cells with corresponding ghost cells in neighboring processors.

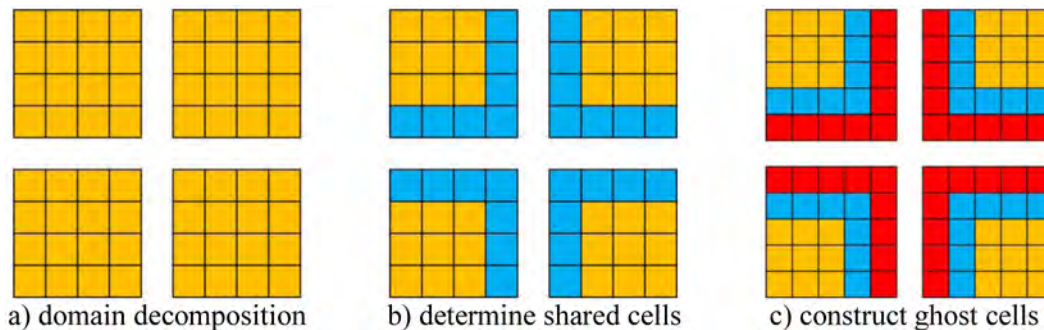


Figure 3—The grids for parallel simulation with MPFA-O



## Numerical results

In this section, we first benchmark the numerical solutions with analytical solutions in single-phase flow to validate the accuracy of the parallel framework. Second, to demonstrate the performance of the OBL method, we perform a benchmark in two-phase flow. In the end, we test the parallel framework with field cases on structured and unstructured grids.

### Benchmark of single-phase flow

Here, we will benchmark the numerical solutions with analytical solutions under a single-phase transient flow state. We apply two kinds of grids to meshing a homogeneous geo-model with a cubic size of  $1 \times 1 \times 1$  m. First, we mesh the domain with four resolutions based on hexahedra shown in Table 1. Second, by splitting the hexahedra grid into six tetrahedrons grids, we generate an unstructured grid. The rock and fluid are incompressible; the reservoir is anisotropic with a full tensor permeability shown below:

$$\mathbf{K} = \begin{bmatrix} 1.0 & 0.5 & 0.0 \\ 0.5 & 1.0 & 0.5 \\ 0.0 & 0.5 & 1.0 \end{bmatrix}. \quad (17)$$

Table 1—Grid dimension and grid size

Grid dimensions	8×8×8	16×16×16	32×32×32	64×64×64
Grid size/m	0.125	0.0625	0.03125	0.015625

The transport equation can be written as:

$$\nabla \cdot (\vec{\mathbf{u}}) = f, \quad (18)$$

where  $f$  is a force term constraint by an analytical solution:

$$P_a = 1.0 + \sin(\pi x)\sin(\pi y)\sin(\pi z)e^{-t}. \quad (19)$$

By defining a function shown in equation (20), we can investigate the accuracy of the numerical solutions.

$$L_{2-integ} = \int_{t=0}^T L_2 dt, \quad L_2 = \sqrt{\sum_{i=1}^N V_i (P_{a-i} - P_{n-i})}. \quad (20)$$

Where  $V_i$  is the volume of the  $i^{th}$  grid;  $P_{a-i}$  is the analytical pressure solution of the  $i^{th}$  block;  $P_{n-i}$  is the numerical pressure solution of the  $i^{th}$  block;  $N$  is the number of blocks.

Through a detailed sensitivity analysis, we find that the optimum values of simulation time and timestep are equal to 5 days and 0.1 days. Prolongation of simulation time or chopping of timestep will barely change the  $L_{2-integ}$ . Finally, we compare the numerical solutions of TPFA and MPFA-O methods using four grid resolutions. From Figure 4, we can see that with the mesh refinement, the solutions of the MPFA-O method converge to a real solution while the TPFA method fails to converge. It demonstrates that our simulator is capable to provide accurate solutions for reservoir simulation in unstructured and full tensor permeability domains.

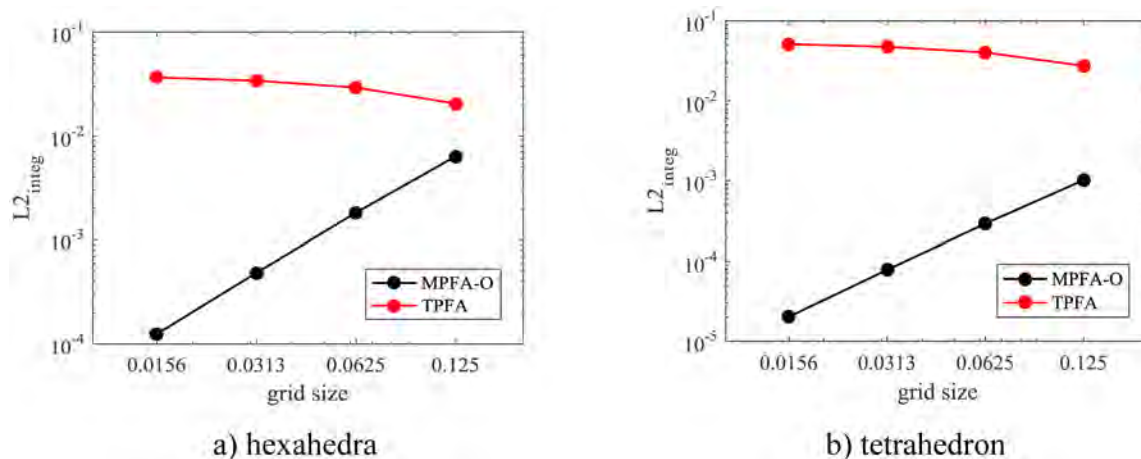


Figure 4— $L_2$ -integ analysis of the MPFA-O and TPFA methods

### Benchmark of multiphase flow

In this section, we will benchmark numerical solutions of two-phase flow with analytical solutions of the Buckley-Leverett equation. Here, the reservoir size is equal to  $10 \times 1 \times 1$  m; the rock and fluid are incompressible; the permeability is 1 mD; the porosity is 0.3; the reservoir is saturated with oil; the viscosities of oil and water are equal to 2 and 1 cP respectively; the relative permeabilities are defined as  $k_{ro} = s_o^2$  and  $k_{rw} = s_w^2$ ; the resolution of the parameter space of each nonlinear known is set as 64. We inject water from the left side and produce oil from the right side with a constant rate equaling  $0.001 \text{ m}^3/\text{day}$  and simulation time equaling 1000 days. We apply hexahedra to meshing the geo-model with grid dimensions equaling to  $1024 \times 5 \times 5$ .

The numerical solutions for pressure and water saturation are shown in Figure 5 and Figure 6. From Figure 6, we can observe a shock of the water saturation. And numerical solution approaches to the real solution which is obtained by solving the Buckley-Leverett equation. By changing the parameters of rock and fluid in the model, we can investigate the effect of the properties on flow behavior which helps us further understand the flow underground.

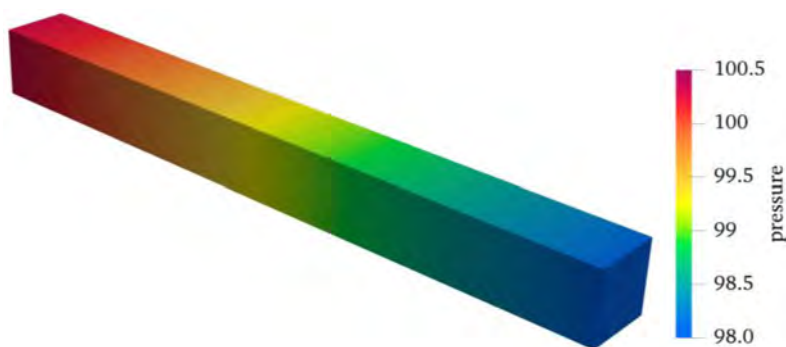


Figure 5—Pressure distribution of the numerical solution

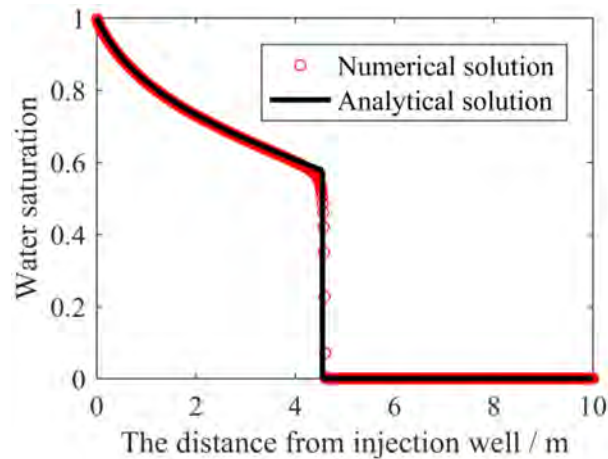


Figure 6—Water saturation of the numerical and analytical solutions

Next, we perform simulations with different grid resolutions including  $64 \times 5 \times 5$ ,  $128 \times 5 \times 5$ ,  $256 \times 5 \times 5$ , and  $512 \times 5 \times 5$ . By defining a function shown in equation (21), we can investigate the effect of grid size on simulation accuracy. As shown in Figure 7, with the mesh refinement, the water saturation approaches to the real solution. It demonstrates that the OBL method is capable to provide accurate and convergent solutions for multiphase flow.

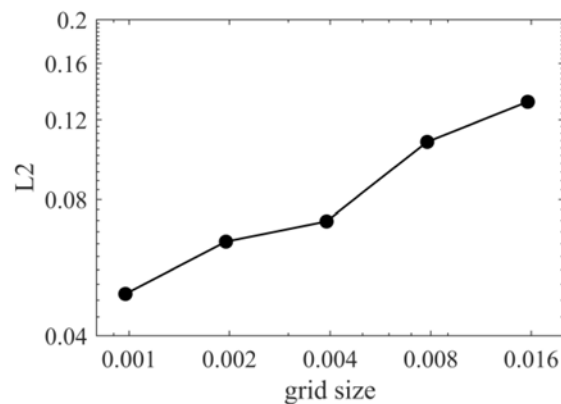


Figure 7—The effect of grid size on the numerical solution

$$L_2 = \sqrt{\sum_{i=1}^N V_i (S_{w-a-i} - S_{w-n-i})^2}. \quad (21)$$

Where  $S_{w-a-i}$  is the analytical water saturation solution of the  $i^{\text{th}}$  block;  $S_{w-n-i}$  is the numerical water saturation solution of the  $i^{\text{th}}$  block.

### Field cases

Since we are still working on a high-performance linear solver [Nardean et al., 2019], the solver applied in this study is just a common one that constrains the simulation efficiency. Thus, in this section, we test a three-dimensional problem based on the top 20 layers of SPE10 reservoir on structured and unstructured grids, which can be taken as a reference for initial testing between the two discretization schemes, and also investigate the scalability of the new parallel simulator.

**Case 1.** The permeability is shown in Figure 8. The rock and fluid are incompressible; the initial pressure is 300 bar; the porosity is homogeneous and equals 0.25; the initial water saturation is 0.2; the viscosities of oil and water are equal to 2 and 1 cP respectively; the relative permeabilities are

defined as  $k_{rw} = [(S_w - S_{wc}) / (1 - S_{wc} - S_{or})]^2$ ,  $k_{ro} = [(S_o - S_{or}) / (1 - S_{wc} - S_{or})]^2$ ,  $S_{wc} = 0.2$ ,  $S_{or} = 0.2$ ; the resolution of the parameter space of each nonlinear known is set as 64; two wells are imposed diagonally with one injector and one producer; the bottom hole pressure of injector is 400 bar; the bottom hole pressure of producer is 200 bar; the simulation time is 5000 days.

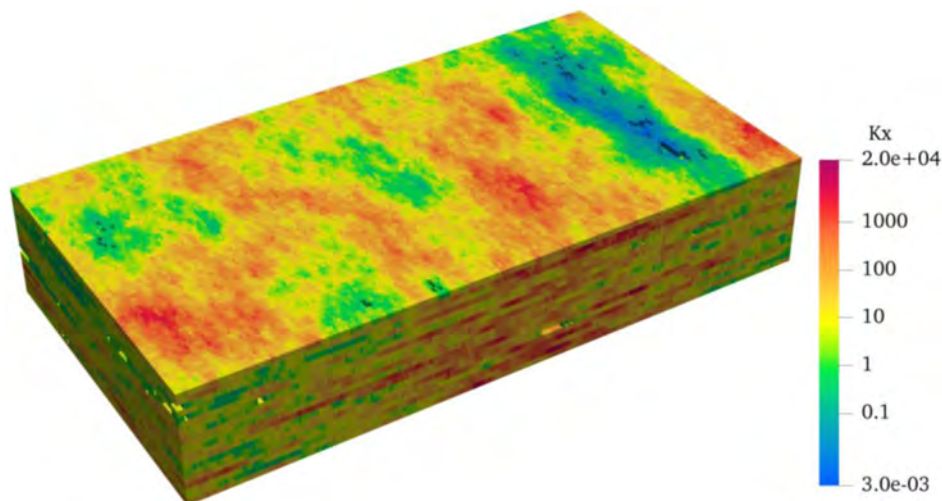


Figure 8—Permeability of the top 20 layers of SPE10 reservoir

We test the MPFA-O and TPFA methods for the strong heterogeneous model which is meshed by hexahedra. As shown in Figure 9, the water saturation distribution is quite complex due to the strong heterogeneities underground. The MPFA-O and TPFA methods provide the same solution since we apply a structured grid and diagonal tensor permeability.

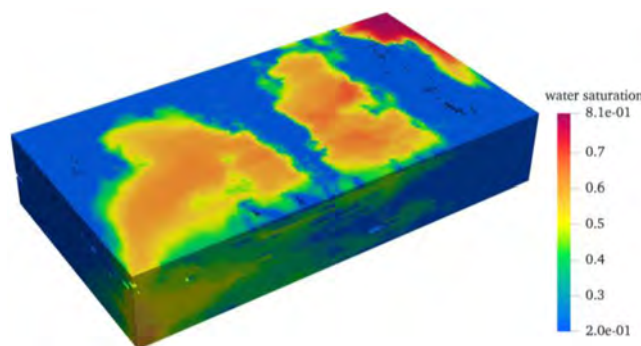


Figure 9—Water saturation distribution after 5000 days (8 cores)

**Case 2.** Here, we bend the geo-model of the previous case and obtain a new model shown in Figure 10. The parameters applied are the same as the last case. From Figure 11a, we can see that the bent strong heterogeneous geo-model introduces a complex flow response and water breakthrough time is 1200 days. By observing the error between MPFA-O and TPFA in Figure 11b, we find that the water breakthrough time is delayed by using the TPFA.

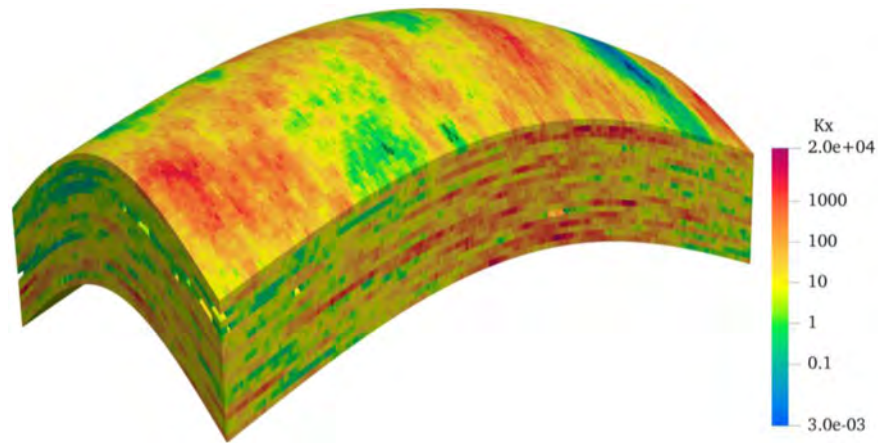


Figure 10—Permeability of the top 20 bent layers of SPE10 reservoir

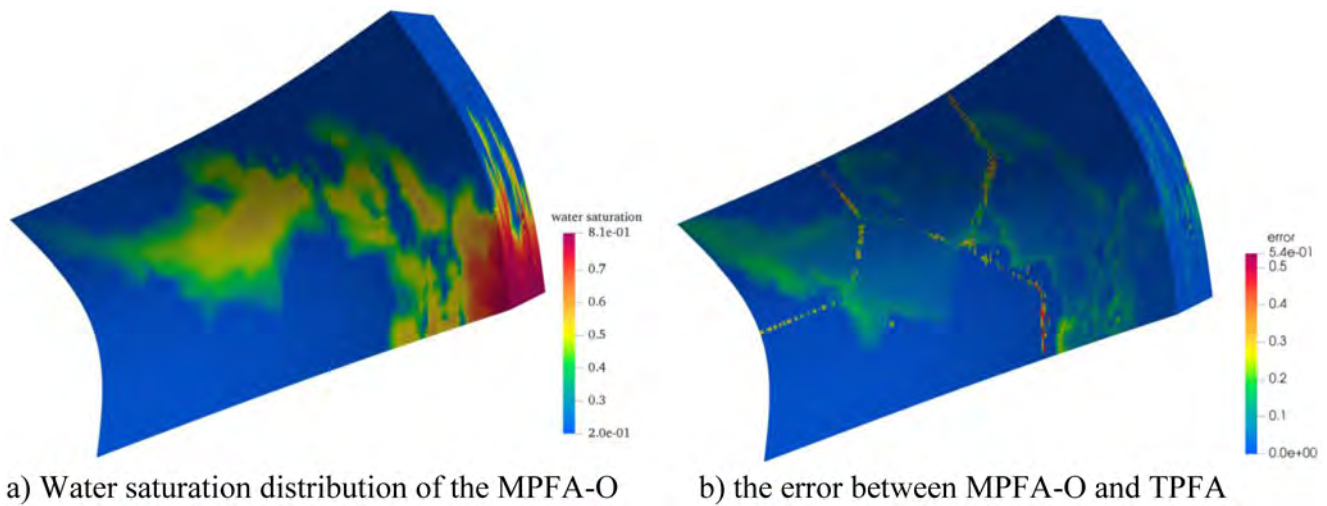


Figure 11—Water saturation distribution and the error between MPFA-O and TPFA after 1200 days

Running the simulation up to 5000 days, we obtain a much more complex water saturation distribution in Figure 12. By performing this simulation on 8, 16, 32, and 64 cores, we can investigate the scalability of the new parallel simulator. As shown in Figure 13, the speedup versus the number of processors demonstrates the strong scalability of this parallel framework for reservoir simulation.



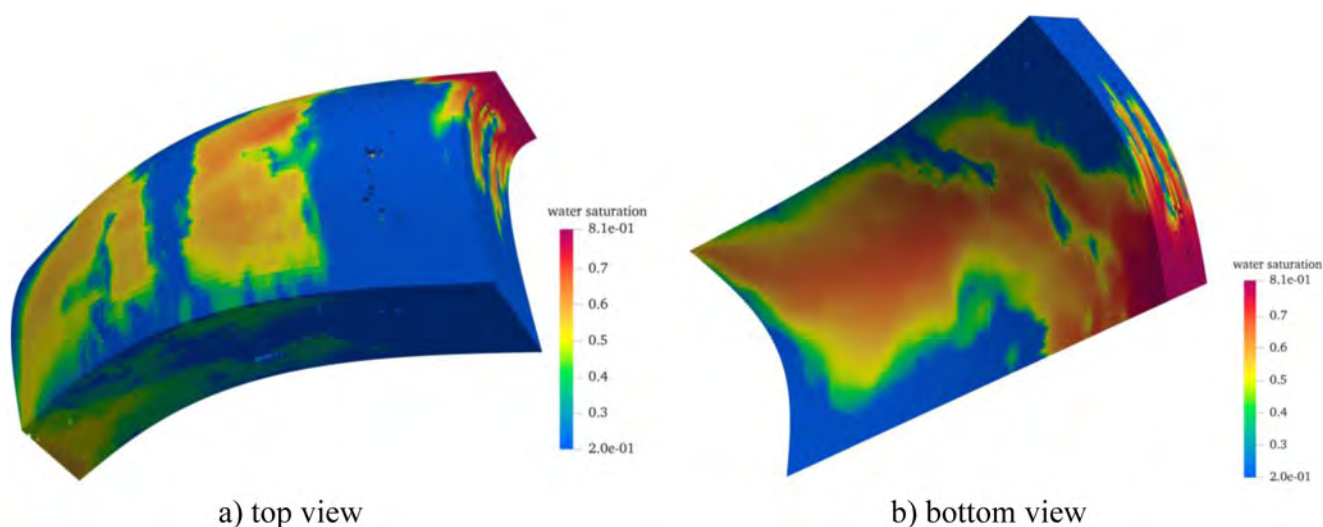


Figure 12—Water saturation distribution of the MPFA-O after 5000 days (8 cores)

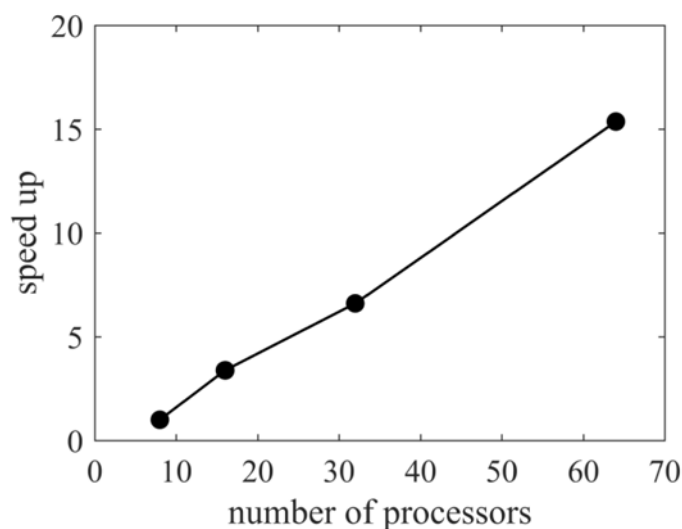


Figure 13—Scalability of the new parallel framework for reservoir simulation

## Conclusions

In this work, an advanced parallel framework for reservoir simulation has been developed. To make the framework flexible for complex geological models and capable to handle full tensor permeability, the MPFA-O method is applied on a general unstructured mesh.

As a general-purpose reservoir simulator, the governing equations are represented by mass-based formulations which could unify different flow models. To overcome the Jacobian assemble hassle and improve the performance of complex phase behavior evaluation, we apply state-of-the-art Operator-Based Linearization (OBL) approach. In the OBL, the governing equations are transformed into an operator form. The state-dependent operators are uniformly discretized in the parameter space of the problem. By computing the values of operators in vertices of hypercubes, we construct a tabulated representation of physics. During a simulation run, once the status falls inside a hypercube, we determine the values of operators and their derivatives by multi-linear interpolation. This way, the phase behavior and property evaluation at each node is reduced to one time only. Besides, the programming complexity or Jacobian assemble is drastically simplified.



In order to simulate results at geological scale, we use massively parallel computations via Message Passing Interface (MPI) to improve the computational efficiency. We benchmark the numerical solutions with analytical solutions of single-phase flow which demonstrates that the parallel framework is capable to provide accurate and convergent solutions for reservoir simulations. Furthermore, to validate the modelling capabilities of multiphase flow, we compare the numerical solutions with analytical solutions obtained by solving the Buckley-Leverett equation. The results demonstrate that our advanced parallel framework for reservoir simulation is capable to handle multiphase flow problems. By using a strong heterogeneous real field geo-model, we run simulations at different numbers of processors. The results demonstrate the strong scalability of the new parallel framework for reservoir simulation.

## Acknowledgment

This publication was supported by the National Priorities Research Program grant NPRP10-0208-170407 from Qatar National Research Fund.

## References

- Aavatsmark, I., Barkve, T., Mannseth, T., 1998. Control-Volume Discretization Methods for 3D Quadrilateral Grids in Inhomogeneous, Anisotropic Reservoirs. *SPE Journal* **3**(02): 146-154.
- Aavatsmark, I., 2002. An introduction to multipoint flux approximations for quadrilateral grids. *Computational Geosciences* **6**: 405-432.
- Abushaikh, A. S., Gosselin, O. R., 2008. Matrix-fracture transfer function in dual-medium flow simulation: Review, comparison, and validation. In Europec/EAGE Conference and Exhibition, 9-12 June 2008, Rome, Italy. SPE-113890-MS.
- Abushaikh, A. S., Blunt M. J., Gosselin O. R., et al., 2015. Interface control volume finite element method for modelling multi-phase fluid flow in highly heterogeneous and fractured reservoirs. *Journal of Computational Physics* **298**: 41-61.
- Abushaikh, A. S., Voskov, D. V., Tchelepi, H. A., 2017. Fully implicit mixed-hybrid finite-element discretization for general purpose subsurface reservoir simulation. *Journal of Computational Physics* **346**: 514-538.
- Abushaikh, A. S., Terekhov K. M., 2018. Hybrid-mixed mimetic method for reservoir simulation with full tensor permeability. In 16th European Conference on the Mathematics of Oil Recovery, 3-6 September, Barcelona, Spain.
- Abushaikh, A. S., Terekhov, K. M., 2020. A fully implicit mimetic finite difference scheme for general purpose subsurface reservoir simulation with full tensor permeability. *Journal of Computational Physics* **406**: 109194.
- Cao, H., 2002. Development of Techniques for General Purpose Simulators. United States: Stanford University.
- Garipov, T. T., Tomin, P., Rin, R. et al., 2018. Unified thermo-compositional-mechanical framework for reservoir simulation. *Computational Geosciences* **22** (4): 1039-1057.
- Garipov, T. T., Karimi-Fard, M., Tchelepi, H. A., 2016. Discrete fracture model for coupled flow and geomechanics. *Computational Geosciences* **20** (1): 149-160.
- Hjeij, D., Abushaikh, A., 2019a. Comparing Advanced Discretization Methods for Complex Hydrocarbon Reservoirs. In SPE Reservoir Characterisation and Simulation Conference and Exhibitions. Society of Petroleum Engineers.
- Hjeij, D., Abushaikh, A., 2019b. An Investigation of the Performance of the Mimetic Finite Difference Scheme for Modelling Fluid Flow in Anisotropic Hydrocarbon Reservoirs. In *SPE EAGE EUROPEC*. Society of Petroleum Engineers.
- Khait, M., Voskov, D. V., 2017. Operator-based linearization for general purpose reservoir simulation. *Journal of Petroleum Science and Engineering* **157**: 990-998.
- Khait, M., Voskov, D. V., 2018a. Operator-based linearization for efficient modeling of geothermal processes. *Geothermics* **74**: 7-18.
- Khait, M., Voskov, D. V., 2018b. Adaptive Parameterization for Solving of Thermal/Compositional Nonlinear Flow and Transport with Buoyancy. *SPE Journal* **23**(02).
- Li, L., Yao, J., Li, Y., 2014. Productivity calculation and distribution of staged multi-cluster fractured horizontal wells. *Petroleum Exploration and Development* **41**(4): 504-508.
- Li, L., Yao, J., Li, Y., 2016. Pressure-transient analysis of CO<sub>2</sub> flooding based on a compositional method. *Journal of Natural Gas Science and Engineering* **33**: 30-36.
- Li L., Voskov D. V., 2018a. Multi-Level Discrete Fracture Model For Carbonate Reservoirs. In 16th European Conference on the Mathematics of Oil Recovery, 3-6 September, Barcelona, Spain.
- Li, L., Voskov, D. V., Yao, J., et al., 2018b. Multiphase transient analysis for monitoring of CO<sub>2</sub> flooding. *Journal of Petroleum Science and Engineering* **160**: 537-554.

- Liu, L., Yao, J., Sun, H., et al., 2018 Compositional modeling of shale condensate gas flow with multiple transport mechanisms. *Journal of Petroleum Science and Engineering* **172**: 1186-1201.
- Nardean, S., Abushaikh, A., Ferronato, M., 2019. A Block Preconditioning Framework for the Efficient Solution of Flow Simulations in Hydrocarbon Reservoirs. In Third EAGE WIPIC Workshop: Reservoir Management in Carbonates, Nov 2019, Doha, Qatar.
- Pruess, K., Oldenburg, C.M., Moridis, G., 1999. TOUGH2 User's Guide, Version 2.0. Report LBNL-43134. Lawrence Berkeley National Laboratory, Berkeley, CA, USA.
- Pruess, K., 2004. The TOUGH Codes--A Family of Simulation Tools for Multiphase Flow and Transport Processes in Permeable Media. *Vadose Zone Journal* **3**(3):738-746.
- Terekhov, K., Vassilevski, Y., 2019. INMOST Parallel Platform for Mathematical Modeling and Applications. In: Voevodin V., Sobolev S. (eds) *Supercomputing. RuSCDays 2018. Communications in Computer and Information Science*, vol **965**. Springer, Cham.
- Voskov, D. V., Tchelepi H. A., 2008. Compositional Space Parametrization for Miscible Displacement Simulation. *Transport in porous media* **75**: 111-128.
- Voskov, D. V., Tchelepi H. A., 2009. Compositional space parameterization: Multicontact miscible displacements and extension to multiple phases. *SPE Journal* **14** (03): 441-449.
- Voskov, D. V., 2012. An extended natural variable formulation for compositional simulation based on tie-line parameterization. *Transport in porous media* **92** (3): 541-557.
- Voskov, D.V., 2017. Operator-based linearization approach for modeling of multiphase multi-component flow in porous media. *Journal of Computational Physics* **337**: 275-288.
- Zaydullin, R., Voskov, D. V., James, S.C. et al., 2014. Fully compositional and thermal reservoir simulation. *Computers and Chemical Engineering* **63**: 51-65.
- Wang, X., Yao, J., Gong, L., 2019. Numerical simulations of proppant deposition and transport characteristics in hydraulic fractures and fracture networks. *Journal of Petroleum Science and Engineering* **183**: 106401.
- Wu, M., Ding, M., Yao, J., et al., 2018. Pressure transient analysis of multiple fractured horizontal well in composite shale gas reservoirs by boundary element method. *Journal of Petroleum Science and Engineering* **162**: 84-101.
- Zhang, N., Abushaikh, A. S., 2019a. An Efficient Mimetic Finite Difference Method For Multiphase Flow In Fractured Reservoirs. In Society of Petroleum Engineers - SPE Europec Featured at 81st EAGE Conference and Exhibition 2019. SPE-195512.
- Zhang, N., Abushaikh, A. S., 2019b. Fully Implicit Reservoir Simulation Using Mimetic Finite Difference Method in Fractured Carbonate Reservoirs. In SPE Reservoir Characterisation and Simulation Conference and Exhibition, 17-19 September, Abu Dhabi, UAE. SPE-196711-MS.